Biochemical and Biophysical Research Communications 505 (2018) 1251–1256

Contents lists available at ScienceDirect

Biochemical and Biophysical Research Communications

journal homepage: www.elsevier.com/locate/ybbrc

Nano-structural analysis of engrafted human induced pluripotent stem cell-derived cardiomyocytes in mouse hearts using a genetic-probe APEX2

Takeshi Hatani [a, b], Shunsuke Funakoshi [b], Thomas J. Deerinck [c, d], Eric A. Bushong [c, d], Takeshi Kimura [a], Hiroshi Takeshima [e], Mark H. Ellisman [c, d, f], Masahiko Hoshijima [c, g, *], Yoshinori Yoshida [b, **]

[a] Department of Cardiovascular Medicine, Graduate School of Medicine, Kyoto University, Kyoto, 606-8507, Japan
[b] Center for iPS Cell Research and Application, Kyoto University, Kyoto, 606-8507, Japan
[c] Center for Research in Biological Systems, University of California at San Diego, La Jolla, CA, 92093, USA
[d] National Center for Microscopy and Imaging Research, University of California at San Diego, La Jolla, CA, 92093, USA
[e] Graduate School of Pharmaceutical Sciences, Kyoto University, Kyoto, 606-8501, Japan
[f] Departments of Neurosciences and Bioengineering, University of California at San Diego, La Jolla, CA, 92093, USA
[g] Department of Medicine, University of California at San Diego, La Jolla, CA, 92093, USA

ARTICLE INFO

Article history:
Received 29 September 2018
Accepted 4 October 2018
Available online 15 October 2018

Keywords:
iPSC-derived cardiomyocytes
Regeneration therapy
Electron microscopy
Cardiac cell transplantation
APEX2

ABSTRACT

Many studies have shown the feasibility of *in vivo* cardiac transplantation of human induced pluripotent stem cell-derived cardiomyocytes (iPSC-CMs) in animal experiments. However, nano-structural confirmation of the successful incorporation of the engrafted iPSC-CMs including electron microscopy (EM) has not been accomplished, partly because identification of graft cells in EM has proven to be difficult. Using APEX2, an engineered ascorbate peroxidase imaging tag, we successfully localized and analyzed the fine structure of sarcomeres and the excitation contraction machinery of iPSC-CMs 6 months after their engraftment in infarcted mouse hearts. APEX2 made iPSC-CMs visible in multiple imaging modalities including light microscopy, X-ray microscopic tomography, transmission EM, and scanning EM. EM tomography allowed assessment of the differentiation state of APEX2-positive iPSC-CMs and analysis of the fine structure of the sarcomeres including T-tubules and dyads.

1. Introduction

Replacement therapies using cells of specific lineages represent a promising strategy to treat a wide range of diseases including congenital and degenerative disorders [1,2]. While the primary interest of studies pursuing cell therapies in human and animal models is the improvement of organ function, the biology of the cell grafts has rarely been pursued in detail. One reason is the absence of methods that would allow these cells to be stably marked for months or years of study after the transplantation. For example, while we and others have been successful in grafting pluripotent stem cell (PSC)-derived cardiomyocytes in animal hearts [3–6], no reports have shown the development of transverse tubules (T-tubules) or "dyads", anatomical hallmark features of mature mammalian ventricular cardiomyocytes (CMs), which are responsible for highly efficient and robust cardiac excitation-contraction (E-C) coupling [7–9].

A monomeric 28-kDa peroxidase reporter, APEX, and its derivative, APEX2, are versatile molecular tags that work for a set of microscopic imaging modalities as well as biochemical proteome profiling [10–12]. Nonetheless, applications have so far been limited mainly to cultured cell experiments, and the efficacy and toxicity of these molecular tags in *in vivo* settings have not been explored months after introduction to a living model. In the current study, we report an imaging strategy that uses APEX2 and robust histone-based marking of the cell nuclei to exam the development of cardiac regulatory machinery *in vivo* in induced pluripotent stem

* Corresponding author. Center for Research in Biological Systems, University of California at San Diego, La Jolla, CA, 92093, USA.
** Corresponding author. Center for iPS Cell Research and Application, Kyoto University, Kyoto, 606-8507, Japan.
E-mail addresses: mhoshijima@gmail.com (M. Hoshijima), yoshinor@cira.kyoto-u.ac.jp (Y. Yoshida).

https://doi.org/10.1016/j.bbrc.2018.10.020
0006-291X/

cell (iPSC)-derived CM (iPSC-CM) grafts. We generated human iPSCs engineered to stably express Histone 2B-fused nuclear-targeted APEX2, induced cardiac differentiation, and engrafted the differentiated cells in a mouse model of acute myocardial infarction. This approach allowed us to identify iPSC-CMs in tissue sections using multi-scale and multimodal imaging methods, including electron and X-ray microscopies (EM and XRM, respectively).

2. Materials and methods

2.1. Generating APEX2 stably expressed iPSCs

We used a human iPSC line, 201B7, into which a human MYH6 promoter driven-EGFP reporter cassette was integrated (MYH6-EIP4) as previously described [4]. An IRES-puromycin cassette was inserted downstream of CAG promoter driven-FLAG-APEX2-H2B. We transfected this APEX2-H2B plasmid and PBase plasmid into MYH6-EIP4 iPSCs with FuGENE® HD Transfection Reagent (Promega, cat. no. E2311). We selected the transfected cells by puromycin and subcloned the transfected cell lines. G band analysis showed that the established APEX2 iPSCs had normal karyotype (Supplementary Fig. 1).

2.2. Cell culture and differentiation of cardiomyocyte, dopaminergic neuron, cortical neuron, and hematopoietic precursor cell in vitro

Human iPSCs were maintained as previously described [4,13]. Cardiac differentiation was induced using an embryoid body (EB) method as previously reported [14–16]. Dopaminergic neuron differentiation was performed by the serum free EB formation method as previously described [17,18]. Cortical neuron and hematopoietic precursor cell differentiation were performed as previously reported [19,20].

2.3. Microarray analysis for iPSCs and iPSC-CMs

For microarray analysis, we used iPSCs and iPSC-CMs at days 7, 14, and 21. iPSC-CMs were sorted by EGFP using fluorescence-activated cell sorter. Cells were lysed with QIAzol Lysis Reagent (Qiagen, cat. no. 79306), and total RNA was extracted using RNeasy Mini Kit (Qiagen, cat. no. 74104). Microarray analysis was carried out using SurePrint G3 Human Gene Expression 8×60K Kit (Agilent Technologies, cat. no. G4851A) with the Microarray Scanner System (Agilent Technologies, cat. no. G2565CA). Data were analyzed by GeneSpring GX version 13.1.1 software (Agilent Technologies). Microarray data are available at the Gene Expression Omnibus (http://www.ncbi.nlm.nih.gov/geo/) under accession no. GSE99470.

2.4. Transplantation of iPS-CMs and in vivo imaging

All experimental protocols were approved by the Kyoto University Animal Experimentation Committee, and the methods were performed in accordance with the Guidelines for Animal Experiments of Kyoto University and the Guide for the Care and Use of Laboratory Animals by the Institute of Animal Resources.

We used male 8–10 week old NOG (NOD/Shi-*scid*/IL-2γ^{null}) immunodeficiency mice. They were intubated and mechanically ventilated under general anesthesia with isoflurane. Myocardial infarctions were induced by ligation of the left anterior descending artery with 8-0 Prolene (Ethicon, cat. no. EP8730H). We injected 20 μL IMDM (Life Technologies, cat. no. 12440-053) containing 1.0×10^6 purified CMs by Hamilton syringe with a 30-gauge needle.

To confirm engraftment, we established a cell line that stably expressed luciferase2. This line was generated by the introduction of a CAG promoter driven-luciferase2 cassette with *PiggyBac* vector in the same way mentioned above. For bioluminescence imaging, mice were under anesthesia with isoflurane, and d-luciferin (SPI, cat. no. XLF-1) was administered at a dose of 200 mg/kg by intraperitoneal injection. Images of mice were captured and luciferase expression level of the engrafted iPSC-CMs was measured by an *in vivo* bioluminescence imaging system (IVIS, Caliper Life Sciences) (Supplementary Fig. 2).

2.5. Immunostaining and microscopy

Immunostaining was carried out as described previously [4,21]. The following primary antibodies were used: mouse anti-FLAG® M2 (Sigma-Aldrich, cat. no. F1804; 1:200), rabbit anti-cardiac troponin I (Santa Cruz Biotechnology, cat. no. sc-15368; 1:100), mouse anti-cardiac troponin T (Thermo Scientific, cat. no. MS-295-P; 1:200), rabbit anti-Nanog (Cell Signaling Technology, cat. no. #4903; 1:50), rabbit anti-TRA-1-60 (Abcam, cat. no. ab174813; 1:100), chicken anti-beta III tubulin (Abcam, cat. no. ab41489; 1:1000), rabbit anti-SATB2 antibody (Abcam, cat. no. ab34735; 1:500), rabbit anti-TBR1 antibody (Abcam, cat. no. ab31940; 1:200), and chicken anti-tyrosine hydroxylase antibody (Abcam, cat. no. ab76442; 1:1000). Secondary antibodies used were as follows: goat anti-mouse IgG-Alexa Fluor® 546 (Life Technologies, cat. no. A-11030; 1:400), goat anti-rabbit IgG-Alexa Fluor® 647 (Life Technologies, cat. no. A-20991; 1:400), goat anti-chicken IgY-Alexa Fluor® 647 (Life Technologies, cat. no. A-21449; 1:400), and goat anti-chicken IgY-Alexa Fluor® 488 (Abcam, cat. no. ab150169; 1:400).

Hoechst 33342 (Life Technologies, cat. no. H3570; 1:10000) was used to counterstain nuclei. The stained cells and tissue sections were visualized using a confocal microscope (Olympus, FV1000) and fluorescence microscope (Keyence, BZ-X710).

2.6. 3,3′-diaminiobenzidine (DAB) staining and preparation of cultured cells for EM

APEX2 iPSCs and their differentiated cells were fixed with glutaraldehyde (Electron Microscopy Sciences, cat. no. 16220) in sodium cacodylate buffer (Electron Microscopy Sciences, cat. no. 11653). A solution of DAB (Sigma-Aldrich, cat. no. D8001) dissolved in HCl was freshly made. After an addition of H_2O_2 solution (Sigma-Aldrich, cat. no. H1009), the DAB-H_2O_2 solution was added to cells for 5–15 min depending on the sample. The generation of DAB precipitates could be monitored by transmitted light microscopy. Post-fixation staining was performed with osmium tetroxide (Electron Microscopy Sciences, cat. no. 19150. The samples were then dehydrated in a graded ethanol (Sigma-Aldrich, cat. no. 459836), infiltrated in Durcupan ACM resin (Sigma-Aldrich, cat. no. 44611-44614), and polymerized in a vacuum oven.

2.7. Preparation of transplanted mouse heart tissues specimens for multimodal microscopic imaging including standard light microscopy, confocal microscopic imaging, XRM and EM

Mouse hearts were perfused in a retrograde way through the ascending aorta with heart solution, followed by paraformaldehyde solution (Electron Microscopy Sciences, cat. no. 15710), and then fixed by formaldehyde. Fixed hearts were embedded with gelatin/albumin, and sliced in 200–300 μm sections using Vibratome (Leica). Sections were fixed using glutaraldehyde, and DAB staining was carried out using the same protocol used for cultured cells. For standard low-voltage transmission EM (TEM) and EM tomography, post-fixation staining was performed with osmium tetroxide. For

scanning EM (SEM), post-fixation staining was performed with osmium tetroxide and potassium ferrocyanide (Sigma-Aldrich, cat. no. 60178). The sections were further incubated with uranyl acetate, dehydrated in a graded ethanol, infiltrated in Durcupan ACM resin, and polymerized in a vacuum oven.

2.8. XRM and EM

XRM was performed using Xradia 510 Versa (Carl Zeiss Microscopy). XRM tilt series were collected at 35–60 kV. Standard TEM imaging was done using JEOL JEM-1200 operated at 80 kV, and FEI Titan 80-300 CTWIN STEM (Thermo Fisher Scientific) operated at 300 kV was used to collect tilt series images for EM tomography by recording images with a 4 K × 4 K charge-coupled device camera (16 bits per pixel). Tomographic reconstruction and the generation of three-dimensional geometric models were carried out using IMOD suite (Boulder Laboratory for 3D Electron Microscopy of Cells, University of Colorado, Boulder, CO). SEM images of sections mounted on silicon wafers were collected using Merlin field emission SEM (Carl Zeiss Microscopy) at 2.0 kV accelerating voltage using backscattered electrons.

3. Results

3.1. Establishment of an APEX2 iPSC line and differentiation into cardiac and other cell lineages

We stably expressed a nuclear-targeted fusion protein, Histone 2B (H2B)-FLAG-APEX2, driven by a CAG promoter in an iPSC line, which was pre-labelled with two genetic markers: EGFP, driven by the cardiac specific human MYH6 promoter, and luciferase, under the control of another copy of the CAG promoter (Fig. 1). The Flag tag was used to demonstrate Flag-APEX2 expression by immunostaining, and EGFP was used to sort iPSC-CMs with a fluorescence-activated cell sorter after differentiation of the iPSCs. Luciferase was used to confirm engraftment of iPSC-CMs by using *in vivo* bioluminescence imaging (Supplementary Fig. 2). This triple-marked iPSC sub-line was named APEX2 iPSC, and DAB reaction confirmed that APEX2 was enzymatically active both in undifferentiated iPSCs and in iPSC-CMs differentiated from APEX2 iPSCs (Fig. 2A–D and Supplementary Fig. 3A-C). Comprehensive transcriptome profiling, cell counting, and the positive expression of cardiac troponin T confirmed that APEX2 expression does not affect iPSC differentiation into a cardiac lineage (Supplementary Fig. 4).

APEX2 iPSCs were also able to differentiate into other cell types, including dopaminergic neurons, cortical neurons, and hematopoietic precursor cells (Supplementary Fig. 5-7). The pluripotency of this APEX2-labelled iPSC cell line was thus ensured.

3.2. Transplantation of APEX2 iPSC-CMs into immune-deficient mouse hearts

APEX2 iPSC-CMs were sorted for cardiac-specific EGFP expression to enhance purity (Supplementary Fig. 3B and C). The purified APEX2 iPSC-CMs were directly transplanted in immuno-deficient NOG mouse hearts with myocardial infraction. Hearts were extracted from host animals 6 months after transplantation.

3.3. Multimodal multi-scale microscopic characterization of APEX2 iPSC-CMs chronically engrafted in mouse hearts

Immunostaining against the Flag tag and cardiac troponin I confirmed efficient engraftment of APEX2 iPSC-CMs (Fig. 3A). For multimodal imaging analysis, the peroxidase reaction was carried out to generate DAB precipitates in APEX2-positive graft cell nuclei, which were readily visible under a standard bright-field light microscope (Fig. 3B). Sections were then treated with OsO_4, embedded in epoxy resin, and examined by high-resolution tomographic XRM. The tomographic images obtained showed that there were a significant amount of sporadic disseminates away from the large cell masses that penetrated into narrow perivascular spaces between host myocardial layers (Fig. 3C, Video 1-3).

Supplementary video related to this article can be found at https://doi.org/10.1016/j.bbrc.2018.10.020.

After mapping APEX2-labelled iPSC-CMs in heart slices by XRM, small resin pieces (approximately 1 × 1 mm^2) containing regions-of-interest (ROIs) identified within the XRM tomographic imaging volumes were excised, and ultra-thin sections (~70–100 nm thickness) were prepared for standard TEM and SEM imaging. For SEM imaging, sections were mounted on silicon wafers and imaged using backscattered electrons. Semi-thin sections (500 nm) were also prepared from the resin pieces containing XRM-defined ROIs for EM tomography [9,21].

TEM and SEM imaging showed modestly organized myofilament bundles in APEX2-positive iPSC-CM grafts (Fig. 4A and B). Stable APEX2 labelling further enabled investigation of the development of E-C coupling apparatuses, which conduct voltage-dependent calcium signaling, in iPSC-CM grafts. Using the EM tomography strategy that was used to reveal novel details of E-C coupling structures in our previous studies [9,21,22], we successfully identified the development of T-tubules and dyads in APEX2-

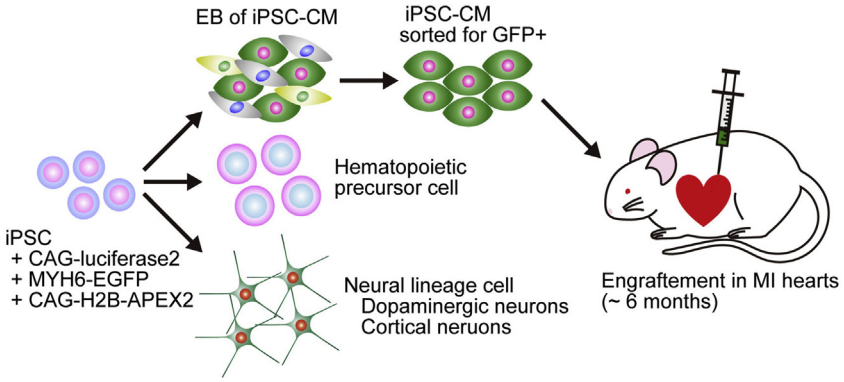

Fig. 1. Outline of this study. Human iPSCs triple-labelled with luciferase 2, EGFP, and Flag-APEX2 were differentiated into a series of distinctive cell lineages including cardiomyocytes(CMs), hematopoietic precursor cells, and two neural lineage cells. iPSC-derived cardiomyocytes (iPSC-CMs) were purified by EGFP with a fluorescence-activated cell sorter, and they were transplanted into immune-deficient mouse hearts with myocardial infarction.

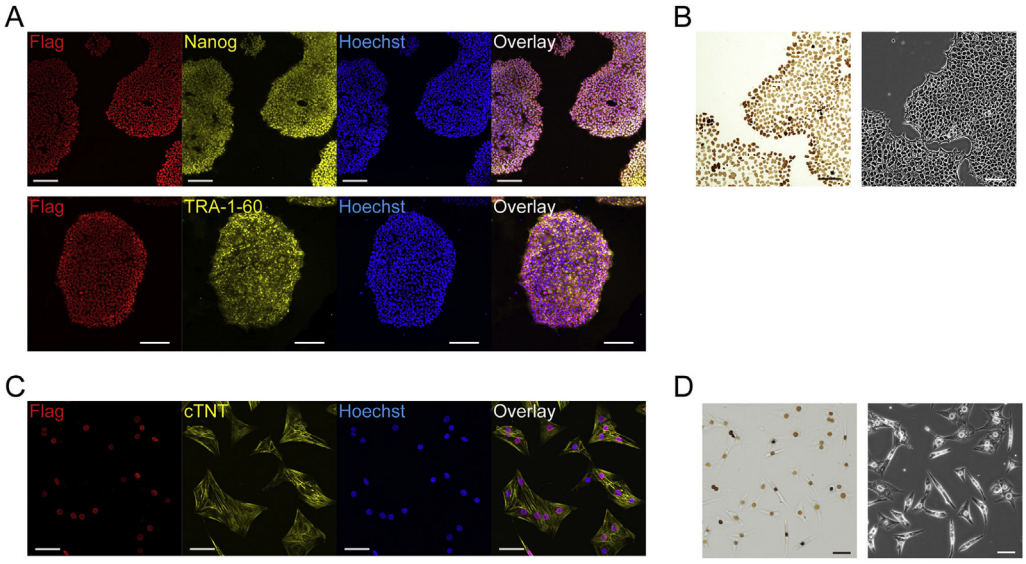

Fig. 2. Established nuclear Flag-APEX2-tagged iPSCs and their differentiation into CMs. A, NANOG and TRA-1-60 are putative genetic markers of stemness and were positive in APEX2 iPSC before differentiation. **B,** DAB reaction verified that peroxidase activity was confined to the nuclei of APEX2 iPSCs. **C,** Full differentiation of APEX2 iPSCs into mature cardiac lineage was evidenced by the expression of cTnT, which was incorporated into well-organized myofilament bundles. **D,** DAB reaction was repeated in APEX2 iPSC-CMs to ensure preserved APEX2 enzymatic activity after cardiac differentiation. In B, D, left: bright field images; right, phase contrast images. Scale bars: A, 200 μm; B, 100 μm; C, 50 μm; D, 50 μm.

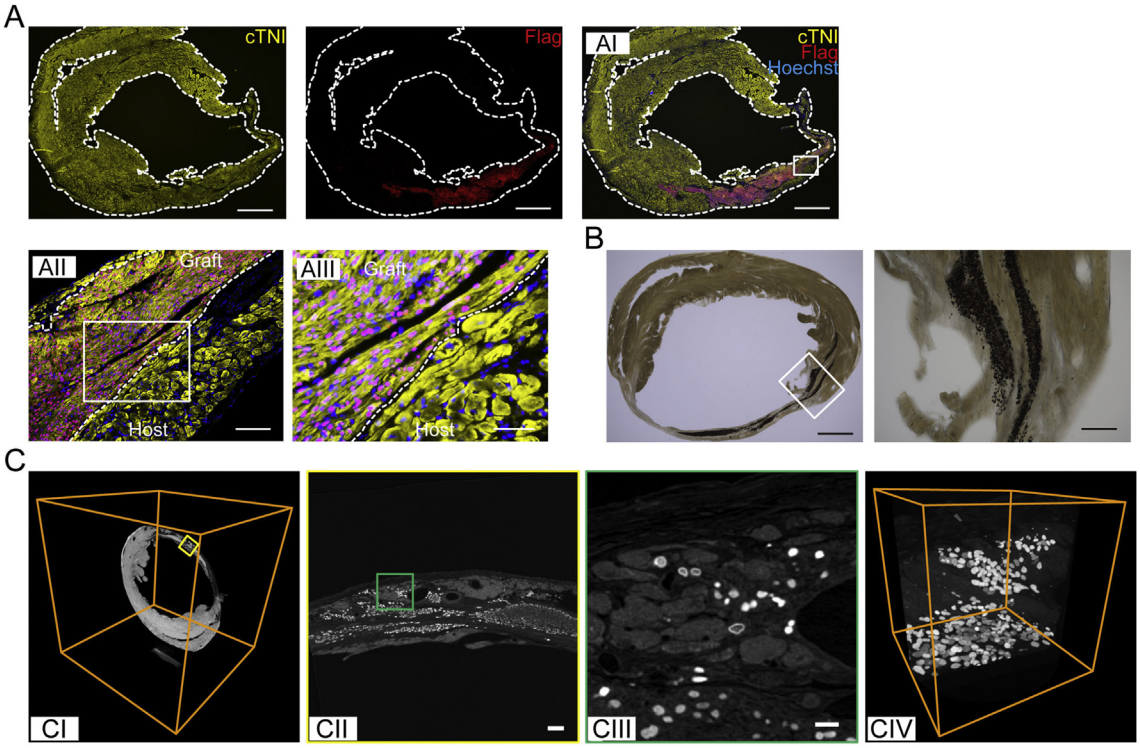

Fig. 3. Light and X-ray microscopic characterizations of nuclear-targeted APEX2 iPSC-CMs chronically engrafted in mouse hearts. A, Flag immuno-staining (red) demonstrates a substantial amount of APEX2 iPSC-CMs residing in a host mouse left ventricular wall with myocardial infarction 6 months after transplantation. AII is high magnification view of a ROI indicated by the white squares in AI. The ROI in AII is further magnified in AIII. cTNI immune-staining (yellow) identify cardiomyocytes. White dotted lines separate host myocardium (cTNI positive, Flag negative) and graft cells (cTNI positive, Flag positive) in AII and AIII. Scale bars: AI, 1000 μm; AII, 100 μm; AIII, 50 μm. **B,** Dark-brown dots observed in the bright-field microscopy images within 200 μm DAB-stained Vibratome heart sections are nuclei of APEX2 iPSC-CMs engrafted for 6 months. The right panel is a high magnification view of the ROI (white square) shown in the left panel. Scale bars: left 1000 μm, right 200 μm. **C**, Reconstructed tomographic XRM images show the heavily stained nuclei of APEX2 iPSC-CM grafts (white spots) with osmium bound to DAB reaction products standing out from the background osmium tissue staining. Three-dimensional distribution of engrafted APEX2 iPSC-CMs among the host CMs were observed. After low-resolution tomograms of the entire cross sections were obtained (CI), resin-embedded ROIs were excised and rescanned at a higher magnification (CII). Smaller ROIs were reassigned and again rescanned to finally achieve sub-micron resolution tomographic images of the grafted cells (CIII and CIV). CI and CIV are maximum intensity projections (MIPs). CII and CIII are ultra-thin multi-planar reconstructions (MPRs) within 200 μm thick tissue specimens. Scale bars, CII, 100 μm; CIII, 20 μm.

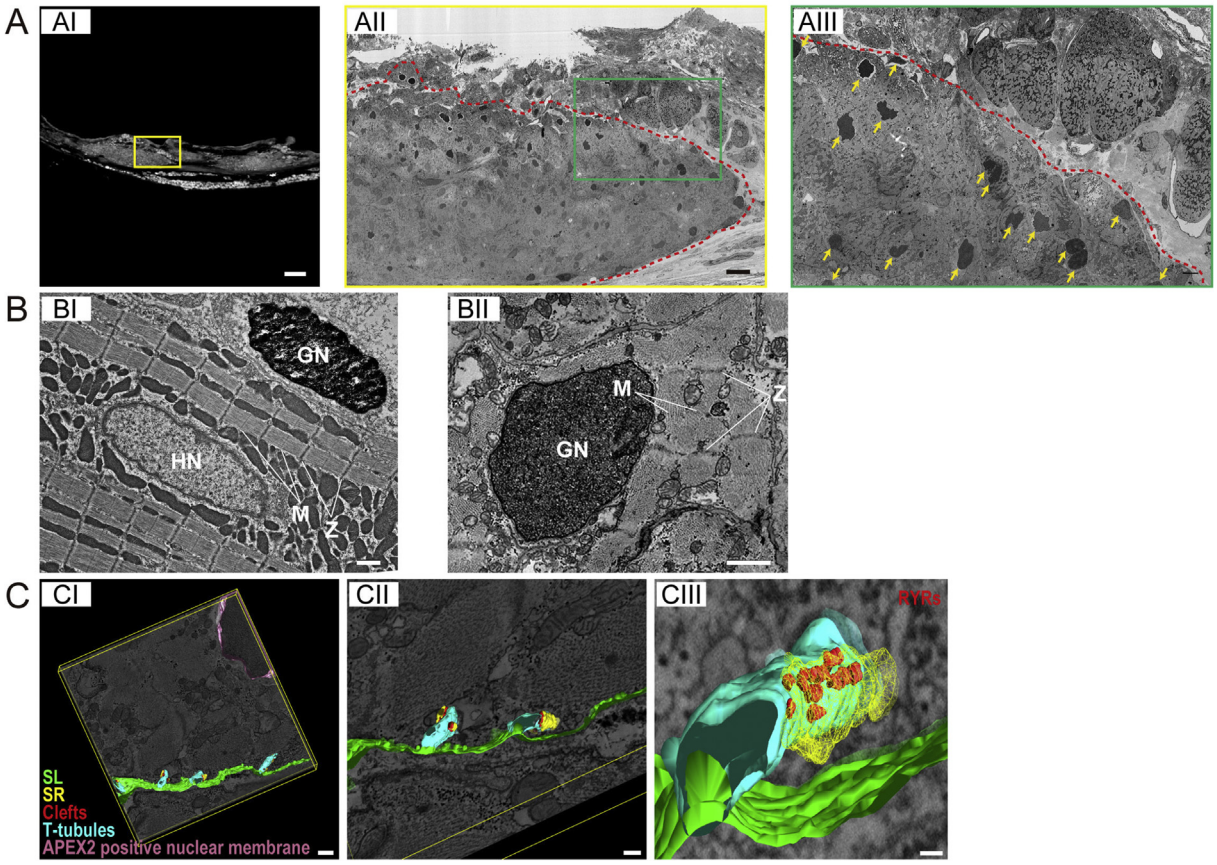

Fig. 4. Electron microscopy characterization of nuclear-targeted APEX2 iPSC-CMs chronically engrafted in mouse hearts. A, Resin specimens examined by XRM (AI) were trimmed at the center of ROIs (yellow square). Ultra-thin sections were made and visualized in SEM on silicon wafers to obtain significantly wide field view images to identify ROIs (AII 30,000 × 20,000 pixels, pixel = 4.5 nm). A thus determined ROI was then rescanned to achieve a higher resolution image (AIII, green square area of AII). The nuclei of APEX2 iPSC-CM grafts were heavily stained by osmium (yellow allows in AIII), which was bound to DAB APEX2 reaction products. The masses of engrafted APEX2 iPSC-CMs were enclosed by red dot lines. (AII and AIII). Scale bars: AI, 200 μm; AII, 20 μm; AIII 5 μm. **B,** Similarly, TEM images of 70–80 nm thick sections prepared from resin pieces containing a ROI determined by XRM. DAB reaction clearly differentiates graft cell nuclei from host CM nuclei (BI). Myofilaments in the graft APEX2 iPSC-CMs were less well organized compared to host CMs. HN; a host cardiomyocyte nucleus; GN; a graft APEX2 iPSC-CM nucleus; Z, Z-line; M, M-line. Scale bars: BI, 1 μm; BII, 1 μm. **C,** an EM tomogram and segmentation of E-C coupling cell apparatus in the tomogram. A semi-thin resin sections (500 nm) containing XRM-defined ROIs was subjected to intermediate high-voltage EM imaging to obtain a set of double-tilt projection images and an EM tomograms was reconstructed using a well-defined computational algorithm. Structures of interest were segmented manually. Computed three-dimensional geometrical meshes show invaginations of T-tubules (blue) from the surface sarcolemma (SL) (green), which are forming primitive forms of dyads with junctional sarcoplasmic reticulum (SR) (yellow). (CI and CII). Dyadic junctional clefts (red) were made between T-tubles and junctional SRs. In a higher resolution image (CIII), 15–20 nm depth junctional clefts are seen between the T-tubules and junctional SRs, and electron dense granular structures, which are assumed to be ryanodine receptors (RyRs), are identified in the clefts (segmented and reconstructed in red). Scale bars: CI, 500 nm; CII, 200 nm; CIII, 100 nm.

positive 6-month iPSC-CM transplants (Fig. 4C, Video 4).

Supplementary video related to this article can be found at https://doi.org/10.1016/j.bbrc.2018.10.020.

4. Discussion

Here we show that APEX2 did not significantly affect cardiac differentiation of iPSCs, nor their proliferation, and was stably expressed in iPSC-CMs over 6 months *in vivo*. Using the APEX2 system, we demonstrate the three-dimensional distribution of engrafted iPSC-CMs in mouse hearts with XRM and also show with EM tomography that T-tubules and dyads emerged in engrafted iPSC-CMs at 6 months after transplantation.

In cell replacement therapy, evaluation of the size, cell number, and other geometric information of engrafted cells is important for functional and structural improvement of target organs. However, in previous reports, information on these factors was limited to two-dimensional low-resolution analysis [3,5,6]. Until present study, there had been no report that successfully imaged the three-dimensional distribution of engrafted cells and their three-dimensional cellular anatomy in heart.

CMs derived from PSCs *in vitro* were previously reported to be immature and more closely resemble embryonic CMs [23]. Therefore, the maturation of engrafted CMs after transplantation is crucial for the recovery of cardiac function. Especially, T-tubules and dyads play important roles in cardiac E-C coupling, and their development is essential for efficient re-muscularization of the injured heart CMs. Furthermore, there are no specific antibodies for T-tubules or dyads. Since membrane junctions such as dyads and peripheral junctions are made in nano-scale, three-dimensional EM technologies are essential for their precise characterization [24]. The enzymatic activity of APEX2 withstands strong EM fixation, which is necessary for excellent ultrastructural preservation. APEX2 can also be used to mark a variety of mammalian organelles and specific proteins. Thus, we propose that experimental *in vivo* applications of APEX2 complement EM imaging and are extremely useful to determine and characterize nano-scale structures of engrafted cells [11].

In summary, we show that APEX2 is a powerful and versatile tool for visualizing specific cell populations, especially genetically engineered stem cell grafts, using multiple multi-scale imaging modalities and for characterizing the long-term fate and biology of

these cells in tissues. Our results also provide the first unequivocal demonstration of the formation of junctional SRs, T-tubules, and dyadic junctional RyR clusters in PSC-derived cardiac cell grafts.

Funding

This work was supported by grants from the Network Program for Realization of Regenerative Medicine from the Japan Agency for Medical Research and Development (Y.Y.), Grants-in-Aid for Scientific Research (Y.Y.) and Core-to-core program (M.H. and H.T.) from the Japanese Society for the Promotion of Science, iPS Cell Research Fund (Y.Y), Human Frontier Science Program (M.H. and H.T.), American Heart Association Western Affiliate (M.H.), and the US NIH to operate the NCMIR for development of and access to advanced technologies and instrumentation under P41 GM103412 (M.H.E).

Acknowledgments

We thank Jeffery Martell, and Alice Ting (Massachusetts Institute of Technology and Stanford University, respectively), and Andrea Thor and other colleagues of NCMIR (National Center for Microscopic Imaging Research, University of California San Diego (UCSD)) for providing materials, their assistance, and invaluable technical advices on APEX2 imaging applications. We greatly appreciate colleagues at our laboratories and the Department of cardiovascular medicine, Kyoto University, for their critical comments. We thank Chikako Okubo, Kenji Miki, Masatoshi Nishizawa, Takeshi Ego, and Kazuhisa Chonabayashi for teaching cardiomyocyte and hematopoietic precursor cell differentiation, Peter Karagiannis for critical reading of the manuscript, and Ikue Takei, Misato Nishikawa, Azusa Inagaki, and Megumi Narita for technical support. We would like to express our heartfelt gratitude to Yoko Uematsu, Azusa Hama, and Sayaka Takeshima for her administrative support.

Appendix A. Supplementary data

Supplementary data to this article can be found online at https://doi.org/10.1016/j.bbrc.2018.10.020.

Transparency document

Transparency document related to this article can be found online at https://doi.org/10.1016/j.bbrc.2018.10.020.

References

[1] S.A. Goldman, Stem and progenitor cell-based therapy of the central nervous system: hopes, hype, and wishful thinking, Cell stem cell 18 (2016) 174–188.
[2] M. Mandai, A. Watanabe, Y. Kurimoto, Y. Hirami, C. Morinaga, T. Daimon, M. Fujihara, H. Akimaru, N. Sakai, Y. Shibata, M. Terada, Y. Nomiya, S. Tanishima, M. Nakamura, H. Kamao, S. Sugita, A. Onishi, T. Ito, K. Fujita, S. Kawamata, M.J. Go, C. Shinohara, K.I. Hata, M. Sawada, M. Yamamoto, S. Ohta, Y. Ohara, K. Yoshida, J. Kuwahara, Y. Kitano, N. Amano, M. Umekage, F. Kitaoka, A. Tanaka, C. Okada, N. Takasu, S. Ogawa, S. Yamanaka, M. Takahashi, Autologous induced stem-cell-derived retinal cells for macular degeneration, N. Engl. J. Med. 376 (2017) 1038–1046.
[3] J.J. Chong, X. Yang, C.W. Don, E. Minami, Y.W. Liu, J.J. Weyers, W.M. Mahoney, B. Van Biber, S.M. Cook, N.J. Palpant, J.A. Gantz, J.A. Fugate, V. Muskheli, G.M. Gough, K.W. Vogel, C.A. Astley, C.E. Hotchkiss, A. Baldessari, L. Pabon, H. Reinecke, E.A. Gill, V. Nelson, H.P. Kiem, M.A. Laflamme, C.E. Murry, Human embryonic-stem-cell-derived cardiomyocytes regenerate non-human primate hearts, Nature 510 (2014) 273–277.
[4] S. Funakoshi, K. Miki, T. Takaki, C. Okubo, T. Hatani, K. Chonabayashi, M. Nishikawa, I. Takei, A. Oishi, M. Narita, M. Hoshijima, T. Kimura, S. Yamanaka, Y. Yoshida, Enhanced engraftment, proliferation, and therapeutic potential in heart using optimized human iPSC-derived cardiomyocytes, Sci. Rep. 6 (2016) 19111.
[5] Y. Shiba, T. Gomibuchi, T. Seto, Y. Wada, H. Ichimura, Y. Tanaka, T. Ogasawara, K. Okada, N. Shiba, K. Sakamoto, D. Ido, T. Shiina, M. Ohkura, J. Nakai, N. Uno, Y. Kazuki, M. Oshimura, I. Minami, U. Ikeda, Allogeneic transplantation of iPS cell-derived cardiomyocytes regenerates primate hearts, Nature 538 (2016) 388–391.
[6] Y.W. Liu, B. Chen, X. Yang, J.A. Fugate, F.A. Kalucki, A. Futakuchi-Tsuchida, L. Couture, K.W. Vogel, C.A. Astley, A. Baldessari, J. Ogle, C.W. Don, Z.L. Steinberg, S.P. Seslar, S.A. Tuck, H. Tsuchida, A.V. Naumova, S.K. Dupras, M.S. Lyu, J. Lee, D.W. Hailey, H. Reinecke, L. Pabon, B.H. Fryer, W.R. MacLellan, R.S. Thies, C.E. Murry, Human embryonic stem cell-derived cardiomyocytes restore function in infarcted hearts of non-human primates, Nat. Biotechnol. 36 (2018) 597–605.
[7] D.M. Bers, Cardiac excitation-contraction coupling, Nature 415 (2002) 198–205.
[8] C. Pinali, A. Kitmitto, Serial block face scanning electron microscopy for the study of cardiac muscle ultrastructure at nanoscale resolutions, J. Mol. Cell. Cardiol. 76 (2014) 1–11.
[9] T. Das, M. Hoshijima, Adding a new dimension to cardiac nano-architecture using electron microscopy: coupling membrane excitation to calcium signaling, J. Mol. Cell. Cardiol. 58 (2013) 5–12.
[10] J.D. Martell, T.J. Deerinck, Y. Sancak, T.L. Poulos, V.K. Mootha, G.E. Sosinsky, M.H. Ellisman, A.Y. Ting, Engineered ascorbate peroxidase as a genetically encoded reporter for electron microscopy, Nat. Biotechnol. 30 (2012) 1143–1148.
[11] S.S. Lam, J.D. Martell, K.J. Kamer, T.J. Deerinck, M.H. Ellisman, V.K. Mootha, A.Y. Ting, Directed evolution of APEX2 for electron microscopy and proximity labeling, Nat. Methods 12 (2015) 51–54.
[12] M. Sastri, M. Darshi, M. Mackey, R. Ramachandra, S. Ju, S. Phan, S. Adams, K. Stein, C.R. Douglas, J.J. Kim, M.H. Ellisman, S.S. Taylor, G.A. Perkins, Sub-mitochondrial localization of the genetic-tagged mitochondrial intermembrane space-bridging components Mic19, Mic60 and Sam50, J. Cell Sci. 130 (2017) 3248–3260.
[13] M. Ohnuki, K. Takahashi, S. Yamanaka, Generation and Characterization of Human Induced Pluripotent Stem Cells, Current Protocols in Stem Cell Biology, Chapter 4, 2009. Unit 4A 2.
[14] L. Yang, M.H. Soonpaa, E.D. Adler, T.K. Roepke, S.J. Kattman, M. Kennedy, E. Henckaerts, K. Bonham, G.W. Abbott, R.M. Linden, L.J. Field, G.M. Keller, Human cardiovascular progenitor cells develop from a KDR+ embryonic-stem-cell-derived population, Nature 453 (2008) 524–528.
[15] K. Miki, K. Endo, S. Takahashi, S. Funakoshi, I. Takei, S. Katayama, T. Toyoda, M. Kotaka, T. Takaki, M. Umeda, C. Okubo, M. Nishikawa, A. Oishi, M. Narita, I. Miyashita, K. Asano, K. Hayashi, K. Osafune, S. Yamanaka, H. Saito, Y. Yoshida, Efficient detection and purification of cell populations using synthetic MicroRNA switches, Cell stem cell 16 (2015) 699–711.
[16] T. Hatani, K. Miki, Y. Yoshida, Induction of human induced pluripotent stem cells to cardiomyocytes using embryoid bodies, Methods Mol. Biol. 1816 (2018) 79–92.
[17] M. Eiraku, K. Watanabe, M. Matsuo-Takasaki, M. Kawada, S. Yonemura, M. Matsumura, T. Wataya, A. Nishiyama, K. Muguruma, Y. Sasai, Self-organized formation of polarized cortical tissues from ESCs and its active manipulation by extrinsic signals, Cell stem cell 3 (2008) 519–532.
[18] A. Morizane, D. Doi, J. Takahashi, Neural induction with a dopaminergic phenotype from human pluripotent stem cells through a feeder-free floating aggregation culture, Methods Mol. Biol. 1018 (2013) 11–19.
[19] T. Kondo, M. Asai, K. Tsukita, Y. Kutoku, Y. Ohsawa, Y. Sunada, K. Imamura, N. Egawa, N. Yahata, K. Okita, K. Takahashi, I. Asaka, T. Aoi, A. Watanabe, K. Watanabe, C. Kadoya, R. Nakano, D. Watanabe, K. Maruyama, O. Hori, S. Hibino, T. Choshi, T. Nakahata, H. Hioki, T. Kaneko, M. Naitoh, K. Yoshikawa, S. Yamawaki, S. Suzuki, R. Hata, S. Ueno, T. Seki, K. Kobayashi, T. Toda, K. Murakami, K. Irie, W.L. Klein, H. Mori, T. Asada, R. Takahashi, N. Iwata, S. Yamanaka, H. Inoue, Modeling Alzheimer's disease with iPSCs reveals stress phenotypes associated with intracellular Abeta and differential drug responsiveness, Cell stem cell 12 (2013) 487–496.
[20] M. Nishizawa, K. Chonabayashi, M. Nomura, A. Tanaka, M. Nakamura, A. Inagaki, M. Nishikawa, I. Takei, A. Oishi, K. Tanabe, M. Ohnuki, H. Yokota, M. Koyanagi-Aoi, K. Okita, A. Watanabe, A. Takaori-Kondo, S. Yamanaka, Y. Yoshida, Epigenetic variation between human induced pluripotent stem cell lines is an indicator of differentiation capacity, Cell stem cell 19 (2016) 341–354.
[21] T. Hayashi, M.E. Martone, Z. Yu, A. Thor, M. Doi, M.J. Holst, M.H. Ellisman, M. Hoshijima, Three-dimensional electron microscopy reveals new details of membrane systems for Ca2+ signaling in the heart, J. Cell Sci. 122 (2009) 1005–1013.
[22] J. Wong, D. Baddeley, E.A. Bushong, Z. Yu, M.H. Ellisman, M. Hoshijima, C. Soeller, Nanoscale distribution of ryanodine receptors and caveolin-3 in mouse ventricular myocytes: dilation of t-tubules near junctions, Biophys. J. 104 (2013) L22–L24.
[23] J.H. van Berlo, J.D. Molkentin, An emerging consensus on cardiac regeneration, Nat. Med. 20 (2014) 1386–1393.
[24] M. Barcena, A.J. Koster, Electron tomography in life science, Semin. Cell Dev. Biol. 20 (2009) 920–930.